

# Thermalization and hydrodynamic long-time tails in a Floquet system

Anne Matthies<sup>1</sup>, Nicolas Dannenfeld<sup>1</sup>, Silvia Pappalardi<sup>1</sup>, and Achim Rosch<sup>1</sup>

<sup>1</sup> *Institute for Theoretical Physics, University of Cologne, 50937 Cologne, Germany*

(Dated: December 20, 2024)

We systematically investigate whether classical hydrodynamic field theories can predict the long-time dynamics of many-particle quantum systems. As an example, we investigate numerically and analytically the time evolution of a chain of spins (or qubits) subject to a stroboscopic dynamics. The time evolution is implemented by a sequence of local and nearest-neighbor gates which conserve the total magnetization. The long-time dynamics of such a system is believed to be describable by a hydrodynamics field theory, which, importantly, includes the effect of noise. Based on a field theoretical analysis and symmetry arguments, we map each operator in the spin model to corresponding fields in hydrodynamics. This allows us to predict which expectation values decay exponentially, and which of them decay with a hydrodynamics long-time tail. We illustrate these findings by studying the time evolution of all 255 Hermitian operators which can be defined on four neighboring sites. We show that all operators not protected by hydrodynamics decay exponentially and investigate a selected set of slowly decaying operators.

Understanding how classical and quantum systems of many particles reach thermal equilibrium has been a venerable question for many decades [1–3]. The universal long-time and large-distance dynamics of large classes of both classical and quantum systems are well understood via *hydrodynamics*, which describes the emergent behavior of conserved densities protected by continuous symmetries [4, 5]. Such theories are believed to apply to thermalizing systems, which approach a finite-temperature thermal state when left alone [6]. There are several successful approaches to hydrodynamics, ranging from fluctuating hydrodynamics [7–10] and macroscopic fluctuation theory [11] to the effective field theory of diffusion [12–15]. These frameworks have remarkable predictive power in describing the long-time behavior of generic hydrodynamics systems, including the corrections at late times [16] or non-linear effects [17].

Hydrodynamic field theories are highly universal as they only depend on the conservation laws in the system [5]. In its simplest setting, there is a single diffusive conservation law. In time-translationally invariant Hamiltonian systems, the energy is always conserved. In a generic spin system with spin-orbit interactions, for example, there is no other conservation law besides energy and one obtains only a single diffusive mode. Two coupled diffusive conservation laws arise, for example, in metals where besides energy also charge is conserved. In fluids, there is additionally momentum conservation, and the Navier-Stokes equations (with added noise terms) define the hydrodynamic field theory. The Navier-Stokes equations in one and two dimensions differ from simpler hydrodynamic theories because non-linearities arising from the coupling of momentum currents to charge or energy are relevant in the renormalization group sense and thus can dominate the behavior at long time and length scales. This leads to dynamics in the Kardar–Parisi–Zhang (KPZ) universality class [10, 18, 19]. The framework of hydrodynamics can be extended to describe also Goldstone modes in systems with spontaneously broken continuous symmetries [5] and even to (classical or quantum) integrable many-particle systems, leading to the so-called generalized hydrodynamics [20–23].

While hydrodynamics is a purely classical theory, it can di-

rectly be used as an effective description of many-body quantum systems at large scales [24–26]. A prototypical example is the so-called quantum quench, the unitary evolution of local observables from an initial pure state, which exhibit slow power-law relaxation,  $\sim t^{-\alpha}$ , even in translationally invariant quantum systems [25]. These ‘hydrodynamics long-time tails’ arise as it takes very long to change the amplitude of fluctuations of conserved densities. Furthermore, hydrodynamics enters in a variety of different quantum phenomena in chaotic systems, ranging from entanglement entropy dynamics [27–31], the scrambling of quantum operators [32–35], spectral statistics [36] and the eigenstate-thermalization hypothesis [37].

There is only a limited number of numerical studies [32, 34, 38] of hydrodynamic long-time tails after a quantum quench starting from Ref. [25]. A recent extensive numerical study by Maceira and Läuchli [39] of quenches in an energy-conserving Hamiltonian system with up to 34 spins studied the relaxation at very long time and, surprisingly, found an exponential relaxation of local observables with a relaxation time growing approximately linearly in system size.

The emergence of hydrodynamics in quantum systems is interesting in its own, but it has regained significant attention recently due to experimental progress in the field of quantum simulation. Remarkable experiments in cold atom platforms have demonstrated the power of analog quantum simulators [40–44], which allows to experimentally explore the continuous time evolution of a given Hamiltonian [45, 46]. More recently, with the advent of quantum computing, significant advances have been made in *digital simulations of time evolution*, where discrete dynamics are implemented via unitary gates acting locally or on nearest neighbors [47, 48]. In this case, even in the absence of energy conservation, hydrodynamics can still emerge, if another conservation law is present, e.g., the conservation of the total magnetization. This case has been studied, for instance, for local random quantum circuits, [27–31, 33, 34, 36, 49–51], where the presence of randomness allowed for exact results. Naturally, these developments raise the question of whether, at large times, i.e., for large circuit depth, the discrete-time evolution in quantum circuits is encoded in hydrodynamic descriptions.

In this work, we perform a detailed analysis of how hydrodynamics emerges in a clean Floquet system, with a discrete translational symmetry. Specifically, we demonstrate how fluctuating hydrodynamics can be used to predict the long-time tails that arise in the quenched dynamics of generic observables  $A$

$$\langle \psi(t_n) | A | \psi(t_n) \rangle, \quad (1)$$

where  $|\psi(t_n)\rangle = U_{\text{FL}}^n |\psi_0\rangle$  is the state evolved at discrete times  $t_n$  with a Floquet operator  $U_{\text{FL}}$  which conserves the total magnetization. These predictions are dictated by a combination of two effects: 1) the interplay of the hydrodynamic modes with symmetries and 2) the role of the initial states. While previous studies on hydrodynamics often focussed on correlation functions of conserved densities, we aim to show that hydrodynamic predictions apply to a much larger set of observables. Thus, we study the time evolution of all 255 possible Hermitian operators  $A$  which can be defined a product of  $X_i, Y_i, Z_i$  and the identity matrix on 4 different sites. For each of these operators we use field theory and symmetry arguments to predict their long-time dynamics. While 128 of them are not protected by any symmetry and hence decay exponentially, we provide a comprehensive analysis of how to understand the impact of the hydrodynamic modes from a derivative expansion. We also discuss the role of the initial states in determining the leading behavior at long times.

Finally, we numerically confirm the validity of our predictions by studying the exact time evolution of time-dependent observables, as described in Eq.(1), for systems with up to  $N = 28$  qubits. We also discuss the influence of finite-size effects, which are mostly exponentially suppressed with  $2^{-N/2}$ . These effects may hide some of the long-time tails in cases where they posses a numerically small prefactor.

Our results emphasize the predictive power of hydrodynamics in describing the long-time behavior of small strings of observables and showcase the importance of symmetries in the characterization of long-time dynamics in digital quantum time evolution.

The rest of the paper is organized as follows. In Sec. I, we introduce the model and discuss the different initial states under analysis. In Sec. II, we provide a summary of fluctuating hydrodynamics and classify the different operators of the spin model to predict their long-time tails. Finally in Sec. III we present the numerical results. We conclude in Sec. IV with a summary and a discussion of the possible failures of hydrodynamics.

## I. MODEL AND CONVENTIONS

We are interested in a generic thermalizing quantum spin system with only one conserved quantity. Our goal is to use the simplest possible setting for equilibration which can also be efficiently simulated numerically. Thus, we chose a system without energy conservation which equilibrates to an infinite temperature state. To break energy conservation, we consider a stroboscopically driven system, which has furthermore the advantage that it can be simulated more easily numerically

(without possible Trotter errors). The time evolution is generated by repeatedly applying a Floquet operator  $U_{\text{FL}}$

$$|\psi_n\rangle = (U_{\text{FL}})^n |\psi_0\rangle. \quad (2)$$

where  $U_{\text{FL}}$  is given by

$$U_{\text{FL}} = e^{-iH_\gamma} e^{-iH_\beta^{\text{even}}} e^{-iH_\beta^{\text{odd}}} e^{-iH_\alpha}. \quad (3)$$

$H_\alpha$  and  $H_\beta$  describe a stroboscopic version of an integrable spin-1/2  $XXZ$ -chain

$$\begin{aligned} H_\alpha &= -\alpha \sum_i Z_i Z_{i+1} \\ H_\beta^{\text{odd}} &= -\beta \sum_i (X_{2i-1} X_{2i} + Y_{2i-1} Y_{2i}) \\ H_\beta^{\text{even}} &= -\beta \sum_i (X_{2i} X_{2i+1} + Y_{2i} Y_{2i+1}), \end{aligned} \quad (4)$$

where  $X_i, Y_i, Z_i$  describe the Pauli matrices at site  $i$  and we consider periodic boundary conditions. For the  $XX$  and  $YY$  couplings even and odd links are treated separately as they do not commute with each other. This allows for an implementation using only 2-qubit gates. The last term ( $H_\gamma$ ) breaks integrability

$$H_\gamma = -\gamma \sum_i Z_i Z_{i+2}. \quad (5)$$

This model only conserves the total  $z$ -magnetization  $M_z = \sum_i Z_i$ .

$$[M_z, U_{\text{FL}}] = \left[ \sum_i Z_i, U_{\text{FL}} \right] = 0. \quad (6)$$

Throughout the paper, we chose the parameters as  $\alpha = 2, \beta = 0.25$  and  $\gamma = 1$ . Experimentally, such time evolutions can be realized directly on quantum computers, where, however, errors and noise terms provide extra complications. As our main goal is to validate and test hydrodynamic approaches, we ignore such effects in the following.

We consider three different initial states  $|\psi_0^{(i)}\rangle$

$$\begin{aligned} |\psi_0^{(1)}\rangle &= (|\uparrow\rangle_Z |\downarrow\rangle_Z)^{\otimes N/2} \\ |\psi_0^{(2)}\rangle &= |+\rangle_X^{\otimes N} \\ |\psi_0^{(3)}\rangle &= (|+\rangle_X |+\rangle_Y |-\rangle_X |-\rangle_Y)^{\otimes N/4}, \end{aligned} \quad (7)$$

describing an initial state  $|\psi_0^{(1)}\rangle$  with staggered magnetization in  $z$ -direction, a state  $|\psi_0^{(2)}\rangle$  with a magnetization in  $+x$ -direction, and a state  $|\psi_0^{(3)}\rangle$  where the magnetization rotates in the  $xy$ -plane. The third state has been chosen as it implements a large and finite spin current in its initial state,  $\langle \psi_0^{(3)} | X_i Y_{i+1} - Y_i X_{i+1} | \psi_0^{(3)} \rangle = 1$  independent of  $i$ . Importantly, all three states are characterized by a discrete translational invariance.

Our goal is to compute and predict the time-dependence of expectation values of observables  $A$ , for long times and large

system sizes based on the time evolution of Eq. (2). We use the notation

$$\langle A(t_n) \rangle^{(m)} \equiv \langle \psi_0^{(m)} | (U_{\text{FL}}^\dagger)^n A (U_{\text{FL}})^n | \psi_0^{(m)} \rangle \quad (8)$$

to denote expectation values of operators computed using  $|\psi_0^{(m)}\rangle$  as an initial state.

## II. FLUCTUATING HYDRODYNAMICS

### A. Fluctuating hydrodynamics as a field theory

Hydrodynamics is a classical effective field theory believed to capture the long-distance large-time dynamics of interacting quantum or classical many body systems close to equilibrium [4, 5]. It builds on the assumption that generic many-particle systems (with the notable exception of integrable systems, many-body localized systems and various types of glasses) relax towards equilibrium starting from an arbitrary excited state. For almost all degrees of freedom, this relaxation is expected to be fast and exponential and the only exceptions are modes protected by continuous symmetries (including Goldstone modes if a continuous symmetry is spontaneously broken). We denote the time scale for local equilibration of these modes by  $\tau^{\text{loc}}$ . In the Floquet system studied by us, there is only a single continuous symmetry, generated by the total magnetization operator  $M_z = \sum_i Z_i$ , Eq. (6). Within the hydrodynamic field theory, we identify  $M_z$  with  $\int dx m(x, t)$ , where  $m(x, t)$  is the local magnetization density. As magnetization cannot be generated or destroyed locally  $m(x, t)$  is a slow mode. As there is no other conservation law, it defines the only slow mode in our system. Our study can be viewed as a test of the assumption underlying hydrodynamics.

The hydrodynamic equation is obtained from the continuity equation for  $m(x, t)$

$$\partial_t m + \nabla j = 0 \quad (9)$$

and an expansion of the current  $j$  in terms of  $m(x, t)$

$$j \approx -D_0 \nabla m - \eta + D_2 m^2 \nabla m + D_3 \nabla^3 m + D_4 \nabla \partial_t m \dots \quad (10)$$

where  $D_0$  is the (magnetic) diffusion constant, while  $D_2, D_3, \dots$  describe non-linear and non-local (in space and time) corrections to the diffusion law. Here we used that  $j$  is odd both under inversion and under  $m \rightarrow -m$ . Importantly, fluctuating hydrodynamics also includes a random noise term,  $\eta(x, t)$  with  $\langle \eta \rangle = 0$ , arising physically from other, non-hydrodynamic degrees of freedom. Using a Gaussian noise

field  $\xi$  with  $\langle \xi(x, t) \xi(x', t') \rangle = \delta(x - x') \delta(t - t')$ , we can use a Taylor expansion similar to Eq. (10) to express

$$\begin{aligned} \eta(x, t) &\approx \sqrt{2C_0} \xi(x, t) \\ &+ C_2 m^2 \xi + C_3 \nabla^2 \xi + C_4 (\xi^3 - 3\langle \xi^2 \rangle \xi) + \dots \end{aligned} \quad (11)$$

where the second line includes symmetry-allowed corrections for non-linear, non-local and non-Gaussian noise. The linearized noisy diffusion equation to leading order in the gradient expansion then reads

$$\begin{aligned} \partial_t m &= D_0 \nabla^2 m + \nabla \eta \\ \langle \eta(x, t) \eta(x', t') \rangle &\approx 2C_0 \delta(x - x') \delta(t - t') \end{aligned} \quad (12)$$

with  $\langle \eta(x, t) \eta(x', t') \rangle \approx 2C_0 \delta(x - x') \delta(t - t')$ . The noise amplitude is (by fluctuation dissipation theorems) proportional to the diffusion constants and the magnetic susceptibility.

The rescaling  $x \rightarrow \tilde{x} = x/\lambda$ ,  $t \rightarrow \tilde{t} = t/\lambda^2$ ,  $\eta \rightarrow \tilde{\eta} = \eta \lambda^{(d+2)/2}$ ,  $m \rightarrow \tilde{m} = m \lambda^{d/2}$  leaves the linearized theory in  $d$  spatial dimension invariant. According to the scaling analysis, all correction to linear hydrodynamics are irrelevant in the renormalization group sense as they are suppressed for large  $\lambda$  when one uses the rescaled coordinates. More specifically, in  $d = 1$  we obtain

$$D_2 \sim C_2 \sim \frac{1}{\lambda}, \quad D_3 \sim D_4 \sim C_3 \sim \frac{1}{\lambda^2}, \quad C_4 \sim \frac{1}{\lambda^3} \quad (13)$$

Thus, their effect vanishes in the long-time limit (see below) and we will need them only to compute subleading corrections to the long-time dynamics of observables.

After rescaling, observables can be expressed in terms of the rescaled variables. As we are interested in the value of observables measured at time  $t$  in the limit of long times, it is useful to choose  $\lambda = \sqrt{t}$  such that  $\tilde{t} = 1$  and then expressing everything in the rescaled variables. For  $d = 1$ , this leads to the following rules for power-counting used heavily in the following

$$\begin{aligned} \nabla_x &= \frac{\nabla_{\tilde{x}}}{t^{1/2}} \sim \frac{1}{t^{1/2}}, & \partial_t &= \frac{\partial_{\tilde{t}}}{t} \sim \frac{1}{t}, \\ m &= \frac{\tilde{m}}{t^{1/4}} \sim \frac{1}{t^{1/4}}, & \eta &= \frac{\tilde{\eta}}{t^{3/4}} \sim \frac{1}{t^{3/4}}. \end{aligned} \quad (14)$$

Such scaling arguments can be used to show that the effects arising from the leading non-linear terms  $D_2$  and  $C_2$  will be suppressed by powers of  $1/\sqrt{t}$  relative to leading terms, see Eq. (13).

In the following, we show in a simple calculation how long-time tails emerge in the linearized theory. The magnetization at time  $t$  is obtained from a straightforward solution of the linearized diffusion equation, Eq. (12)

$$m(x, t) = \int_{-\infty}^{\infty} dx' G(x - x', t) m(x', 0) + \int_{-\infty}^{\infty} dx' \int_0^t dt' G(x - x', t - t') \nabla \eta(x', t') \quad (15)$$

where  $G(x, t) = \theta(t) e^{-x^2/(4D_0 t)} / (4\pi D_0 t)^{1/2}$  is the Green's function of the diffusion equation with Fourier transformation

$G_k(t) = \theta(t)e^{-D_0k^2t}$ . We describe the noise by  $\langle \eta(x, t)\eta(x', t') \rangle = \delta(t - t')C^\eta(x - x')$ . Furthermore, we assume that the initial correlations at  $t = 0$  are given by  $\langle m(x_1, 0)m(x_2, 0) \rangle = C(x_1 - x_2)$ , where  $C$  is a function that depends on the initial state. This allows to calculate the equal-time correlation function at time  $t$

$$\begin{aligned}
\langle m(x, t)m(\tilde{x}, t) \rangle &= \int_{-\infty}^{\infty} dx_1 \int_{-\infty}^{\infty} dx_2 G(x - x_1, t)G(\tilde{x} - x_2, t)\langle m(x_1, 0)m(x_2, 0) \rangle \\
&+ \int_{-\infty}^{\infty} dx_1 \int_{-\infty}^{\infty} dx_2 \int_0^t dt_1 \int_0^t dt_2 G(x - x_1, t - t_1)G(\tilde{x} - x_2, t - t_2)\langle \nabla\eta(x_1, t_1)\nabla\eta(x_2, t_2) \rangle \\
&= \int \frac{dk}{2\pi} G_k(t)G_{-k}(t)C_k e^{i(x-\tilde{x})k} + \int_0^t dt_1 \int \frac{dk}{2\pi} k^2 G_k(t - t_1)G_{-k}(t - t_1)C_k^\eta e^{i(x-\tilde{x})k} \\
&= \int \frac{dk}{2\pi} e^{-2D_0k^2t} C_k e^{i(x-\tilde{x})k} + \int \frac{dk}{4\pi D_0} \left(1 - e^{-2D_0k^2t}\right) C_k^\eta e^{i(x-\tilde{x})k} \\
&= \frac{C^\eta(x - \tilde{x})}{2D_0} + \theta(t) \frac{e^{-(x-\tilde{x})^2/(8D_0t)}}{\sqrt{8\pi D_0t}} \left[ \left( C_{k=0} - \frac{C_{k=0}^\eta}{2D_0} \right) + \frac{(4D_0t - (x - \tilde{x})^2)}{32D_0^2t^2} \left( C_{k=0}'' - \frac{C_{k=0}^{\prime\prime\eta}}{2D_0} \right) + \dots \right]
\end{aligned} \tag{16}$$

where we used that  $\langle m(x)m(x') \rangle = \langle m(x')m(x) \rangle$  and therefore  $C(x) = C(-x)$  for a translationally invariant system. Thus, the Fourier transform  $C_k = C_{-k}$  has no odd components in  $k$  independent of the symmetries of the initial state. Here,  $\frac{C^\eta(x-\tilde{x})}{2D_0}$  can be identified with the steady-state correlation function, which is obtained for  $t \rightarrow \infty$ . Hydrodynamic long-time tails arise whenever the initial correlation functions and the steady-state correlation function are different. If the  $k = 0$  correlations,  $C_{k=0} = \int C(x)dx$ , of the initial state differ from the correlations  $\frac{C_{k=0}^\eta}{2D_0}$ , one obtains, for example,

$$\langle m(x, t)^2 \rangle \sim \frac{1}{\sqrt{t}}, \quad \langle (\nabla m(x, t))^2 \rangle \sim \frac{1}{t^{3/2}}. \tag{17}$$

Only by diffusive processes the fluctuations of the magnetization can be readjusted, which leads to pronounced long-time tails.

## B. Mapping to hydrodynamics

To be able to use the conventional units for space and time, we first introduce a lattice constant  $a$  and also associate each unitary with a time scale  $T$ , which is its duration. We denote the position of spin  $j$  by  $x_j = aj$  and the time after the application of  $n$  unitaries by  $t_n = nT$ . As  $T$  and  $a$  are simply conventions, their value is irrelevant (and can also be set

to 1). We employ a Heisenberg picture for operators  $A$  with  $A(t_n) = (U^\dagger)^n A U^n$ .

A mapping of the quantum system to fluctuating hydrodynamics is only possible in the limit  $t_n \gg \tau^{\text{loc}}$ , where  $\tau^{\text{loc}}$  is the local equilibration time, which gives an upper limit of the decay-time of all non-hydrodynamic modes. The existence of such a time-scale is an assumption, which we will test numerically.

The first target of the hydrodynamic equation is to compute expectation values of products of operators  $Z_i$ . We will focus on equal-time expectation values after initializing the system with a wave function  $|\Psi\rangle$  with  $\langle A(t_n) \rangle = \langle \psi | A(t_n) | \psi \rangle$ . Thus, hydrodynamics should predict in the long-time limit

$$\begin{aligned}
&\langle Z_{i_1}(t_n)Z_{i_2}(t_n)\dots Z_{i_m}(t_n) \rangle \\
&= \langle m(x_{i_1}, t_n)m(x_{i_2}, t_n)\dots m(x_{i_m}, t_n) \rangle
\end{aligned} \tag{18}$$

where  $\langle \dots \rangle$  on the left-hand side denotes the quantum mechanical expectation value  $\langle \psi_0 | \dots | \psi_0 \rangle$ , while  $\langle \dots \rangle$  on the right side is computed from a solution of the nonlinear hydrodynamic equation using an average over all noise configurations. Here, the initial conditions should be set by matching the correlations and their time derivatives at an initial time  $t_{\text{ini}} \gg \tau^{\text{loc}}$ .

While the mapping of products of  $Z_i$  to the slow mode  $m(x)$  follows from the definition of  $m$ , for any other operator such a mapping is not straightforward. However, we can expect that for an operator  $A_i(t_n)$ , where  $i$  denotes the position, a Taylor expansion exist of the following form

$$\begin{aligned}
\langle A_i(t_n) \rangle \approx & \left\langle \gamma^{(0,0)} + \int dx_1 dt_1 \gamma_{x_1-x_i, t_1-t_n}^{(1,0)} m(x_1, t_1) + \int dx_1 dt_1 \gamma_{x_1-x_i, t_1-t_n}^{(0,1)} \eta(x_1, t_1) \right. \\
& + \int dx_1 dt_1 dx_2 dt_2 \gamma_{x_1-x_i, x_2-x_i, t_1-t_n, t_2-t_n}^{(1,1)} m(x_1, t_1) \eta(x_2, t_2) \\
& + \int dx_1 dt_1 dx_2 dt_2 \gamma_{x_1-x_i, x_2-x_i, t_1-t_n, t_2-t_n}^{(2,0)} m(x_1, t_1) m(x_2, t_2) \\
& \left. + \int dx_1 dt_1 dx_2 dt_2 \gamma_{x_1-x_i, x_2-x_i, t_1-t_n, t_2-t_n}^{(0,2)} \eta(x_1, t_1) \eta(x_2, t_2) + \dots \right\rangle \quad (19)
\end{aligned}$$

where the function  $\gamma^{(i,j)}$  are expected to decay exponentially as function of distance and time.

Note that the coefficients of the Taylor expansion are independent of the initial condition of the system (which is encoded in the initial condition of the hydrodynamic equation as discussed above).

As a next step, one can then perform a Taylor expansion of  $m(x_j, t_j)$  around the point  $x_i, t_n$  to arrive at

$$\begin{aligned}
\langle A_i(t_n) \rangle \approx & \left\langle \gamma^{(0,0)} + \gamma_0^{(1,0)} m(x_i, t_n) + \gamma_1^{(1,0)} \nabla m(x_i, t_n) + \gamma_2^{(1,0)} \partial_t m(x_i, t_n) + \dots + \gamma_0^{(0,1)} \eta(x_i, t_n) + \gamma_1^{(0,1)} \nabla \eta(x_i, t_n) + \dots \right. \\
& + \gamma_0^{(1,1)} m(x_i, t_n) \eta(x_i, t_n) + \gamma_1^{(1,1)} \nabla (m(x_i, t_n) \eta(x_i, t_n)) + \dots + \gamma_0^{(2,0)} (m(x_i, t_n))^2 + \gamma_1^{(2,0)} \nabla (m(x_i, t_n))^2 + \dots \\
& \left. + \gamma_0^{(0,2)} (\eta(x_i, t_n))^2 + \gamma_1^{(0,2)} \nabla (\eta(x_i, t_n))^2 + \dots \right\rangle \\
= & \sum_{i,j} \left\langle \gamma_0^{(i,j)} m(x_i, t_n)^i \eta(x_i, t_n)^j + \gamma_1^{(i,j)} \nabla (m(x_i, t_n)^i \eta(x_i, t_n)^j) + \gamma_2^{(i,j)} \partial_t (m(x_i, t_n)^i \eta(x_i, t_n)^j) + \dots \right\rangle, \quad (20)
\end{aligned}$$

where the real-valued prefactors can be computed from the functions  $\gamma^{(i,j)}$  defined in Eq. (19). One gets, for example,  $\gamma_1^{(1,0)} = \int dx_1 dt_1 \gamma_{x_1-x_i, t_1-t_n}^{(1,0)} (x_1 - x_i) = \int dx dt \gamma_{x,t}^{(1,0)} x$ .

The coefficients of the Taylor expansion are strongly restricted by symmetries and, as we argue below, also by the fact that our system approaches an infinite-temperature steady state. We will work out the corresponding constraints for the dynamics in the following section.

### C. Predicting long-time tails by classifying operators

We have classified all 255 possible Hermitian operators  $B_j$  which can be written as a product of  $X_i, Y_i, Z_i$  (and the identity matrix) on four neighboring sites  $i, i+1, i+2, i+3$ . Table I shows how we can map the microscopic operators to objects in the field theory. For definiteness, we chose a convention where  $i = 4n$  is always a multiple of 4. These 255 operators form (together with the identity) a complete basis of Hermitian operators on four neighboring sites. Thus, they can be used to reconstruct the 4-site reduced density matrix. Using that  $\text{tr}(B_i B_j) = \delta_{i,j} 2^4$  for our operators, one obtains

$$\rho^{\text{red}} = \frac{1}{2^4} \sum_{j=0}^{255} B_j \langle B_j \rangle. \quad (21)$$

where  $B_0$  is the identity matrix.

To construct the table I and to predict long-time tails, we use a combination of seven different arguments. The first four are independent of the initial state, the last three take properties of the initial state into account.

#### 1. Constraints arising from symmetries of the time evolution operator

(i) The effective field theory is rotation invariant by spin rotations around the z-axis. Thus, only operators which are spin-rotation invariant, can be described by this theory. Therefore, we symmetrize each operator  $A$  using the generator of rotations  $M_z = \sum Z_i$ ,

$$A|_{\text{sym}} = \int_0^{2\pi} \frac{d\alpha}{2\pi} e^{i\alpha M_z/2} A e^{-i\alpha M_z/2} \quad (22)$$

Three examples of symmetrized operators are

$$\begin{aligned}
X_i X_{i+1}|_{\text{sym}} &= \frac{1}{2} (X_i X_{i+1} + Y_i Y_{i+1}) \\
X_i Y_{i+1}|_{\text{sym}} &= \frac{1}{2} (X_i Y_{i+1} - Y_i X_{i+1}) \\
X_i Y_j Z_k|_{\text{sym}} &= \frac{1}{2} (X_i Y_j - Y_i X_j) Z_k. \quad (23)
\end{aligned}$$

If  $A|_{\text{sym}} = 0$ , the operator is not protected by conservation laws and is expected to decay exponentially. This happens if the total number of  $X$  and  $Y$  operators is odd and applies to 128 of the 255 operators considered by us. It is a crucial assumption of hydrodynamics that all operators, unprotected by slow modes, decay exponentially, which we will test numerically below. More generally, we expect an exponential decay for all expectation values of the type

$$\langle A - A|_{\text{sym}} \rangle \sim e^{-\Gamma t}. \quad (24)$$

Examples of exponentially decaying operators are  $X_i, Y_i, X_i Y_{i+1} X_{i+2}$ , or  $X_i Y_j + Y_i X_j$ .

TABLE I. Classification of all 255 range-4 operators  $B_i$ . Half of those operators (128) are not protected by hydrodynamics,  $B_i|_{\text{sym}} = 0$  and thus decay exponentially, see text and Fig. 2. The remaining 127 operators can be sorted into 9 sets of operators.  $n_{\text{op}}$  gives the number of operators in each set. The column labeled  $R_{\pi\hat{x}}$  shows whether the operator  $B_i|_{\text{sym}}$  is even or odd under rotations by  $\pi$  around the  $\hat{x}$ . This determines whether it contains an even or odd power of  $m$  within hydrodynamics. Similarly, the next column labeled  $I_L$  identifies which operators  $B_i|_{\text{sym}}$  are even or odd under inversion on a link. “–” indicates that the operator is neither even or odd. Even (odd) operators contain an even (odd) number of gradients. Based on these symmetries, one can find the leading operator in the field theory, listed in the next column. However, whether these operators obtain a finite expectation value or not depends on the initial condition. Therefore, for the three initial conditions considered in our paper, the last three pairs of columns give an example of the most relevant operator with a finite expectation value. The entry – denotes that due to symmetry no such operator exists.

	operators	$n_{\text{op}}$	$R_{\pi\hat{x}}$	$I_L$	field theory leading	$ \psi_0^{(1)}\rangle$ (staggered) leading	$ \psi_0^{(2)}\rangle$ (x-pol.) leading	$ \psi_0^{(3)}\rangle$ (current) leading
1	$Z_i$	4	–1	–	$m$	$(\nabla m)^3$	–	$(\nabla m)^3$
2	$Z_i Z_{i+1}, Z_i Z_{i+3}$	4	1	1	$m^2$	$m^2$	$m^2$	$m^2$
3	$Z_i Z_{i+2}$	2	1	–	$m^2$	$m^2$	$m^2$	$m^2$
4	$Z_i Z_{i+n_1} Z_{i+m}$	4	–1	–	$m^3$	$(\nabla m)^3$	–	$(\nabla m)^3$
5	$Z_i Z_{i+1} Z_{i+2} Z_{i+3}$	1	1	1	$m^4$	$m^4$	$m^4$	$m^4$
6	$X_i X_{i+1}, Y_i Y_{i+1}, X_i X_{i+3}, Y_i Y_{i+3}$ $X_i X_{i+1} X_{i+2} X_{i+3}, Y_i Y_{i+1} Y_{i+2} Y_{i+3}$ $A_i B_{i+1} B_{i+2} A_{i+3}, A \neq B \in \{X, Y, Z\}$	16	1	1	$(\nabla m)^2$	$(\nabla m)^2$	$(\nabla m)^2$	$(\nabla m)^2$
7	$X_i X_{i+2}, Y_i Y_{i+2}$ $A_i B_{i+1} A_{i+2} B_{i+3}, A \neq B \in \{X, Y, Z\}$ $A_i A_{i+1} B_{i+2} B_{i+3}, A \neq B \in \{X, Y, Z\}$ $X_i Y_{i+k} Z_{i+n}, Y_i X_{i+k} Z_{i+n}$	40	1	–	$m \nabla m$	$(\nabla m)^2$	$(\nabla m)^2$	$(\nabla m)^2$
8	$X_i Y_{i+1}, Y_i X_{i+1}, X_i Y_{i+3}, Y_i X_{i+3}$ $X_i Z_{i+1} Z_{i+2} Y_{i+3}, Y_i Z_{i+1} Z_{i+2} X_{i+3}$ $Z_i X_{i+1} Y_{i+2} Z_{i+3}, Z_i Y_{i+1} X_{i+2} Z_{i+3}$	12	–1	–1	$\nabla m$	$(\nabla m)^3$	–	$(\nabla m)^3$
9	$X_i Y_{i+2}, Y_i X_{i+2}$ $X_i X_{i+n} Z_{i+m}, Y_i Y_{i+n} Z_{i+m}$ $X_i X_{i+k} X_{i+n} Y_{i+m}, Y_i Y_{i+k} Y_{i+n} X_{i+m}$ $X_i Y_{i+1} Z_{i+2} Z_{i+3}, Y_i X_{i+1} Z_{i+2} Z_{i+3}$ $Z_i Z_{i+1} X_{i+2} Y_{i+3}, Z_i Z_{i+1} Y_{i+2} X_{i+3}$ $Z_i X_{i+1} Z_{i+2} Y_{i+3}, Z_i Y_{i+1} Z_{i+2} X_{i+3}$ $X_i Z_{i+1} Y_{i+2} Z_{i+3}, Y_i Z_{i+1} X_{i+2} Z_{i+3}$	44	–1	–	$\nabla m$	$(\nabla m)^3$	–	$(\nabla m)^3$

(ii) As a second step, we consider, how the operators transform under spin rotation by  $\pi$  around the  $x$  axis

$$A \rightarrow R_{\pi\hat{x}}^{-1} A R_{\pi\hat{x}}, \quad R_{\alpha\hat{n}} = e^{-i\alpha \sum \hat{n} \cdot \sigma_i / 2} \quad (25)$$

If  $A$  is even or odd under this transformation, its expansion into hydrodynamic modes will contain an even or odd power of  $m$ , respectively, as  $m$  is odd under this symmetry. More precisely, also  $\eta$  is odd under this symmetry, but we omit terms containing powers of  $\eta$  in our analysis as  $\eta$  correlators are local in time.

(iii) Next, we have to investigate how an operator  $A|_{\text{sym}}$  transforms under the spatial link-inversion symmetry  $I_L$  when we choose the link between  $i_0$  and  $i_0+1$  as a center of inversion

$$I_L : \quad i \rightarrow (2i_0 + 1) - i. \quad (26)$$

Note that spatial inversion centered on a site,  $i \rightarrow 2i_0 - i$ , is *not* a symmetry of our time evolution operator, as we apply the  $XX$  and  $YY$  operators in Eq. (3) first on odd and only later on even links. If the operator  $A|_{\text{sym}}$  is even or odd under this operation, it will contain an even or odd number of gradients within the effective field theory, respectively. Often,  $A|_{\text{sym}}$  will, however, be neither symmetric nor antisymmetric under link inversion. For example,  $X_1 X_3$  transforms as  $X_1 X_3 \rightarrow$

$X_2 X_4$  under link-inversion, but translation by a single site is not a symmetry of our time-evolution operator. In this case, we have to allow for both even and odd powers of gradients in the Taylor expansion.

(iv) Beyond symmetry, we have to take into account some special properties of our infinite-temperature fixpoint. Here, it is useful to consider a state with finite magnetization in the limit  $t \rightarrow \infty$ . As this is an infinite temperature state, all sites are uncorrelated and  $\langle X_i \rangle = \langle Y_i \rangle = 0$  while  $\langle Z_i \rangle = \langle m \rangle$ . We can use that to compute exactly expansion coefficients  $\gamma_0^{(n)}$ , the prefactors of  $m^n$ , in the Taylor expansion of operators in Eq. (20). Matching the left and the right side in

$$\lim_{t \rightarrow \infty} \langle A \rangle = \gamma_0^{(n)} \langle m^n \rangle_{T \rightarrow \infty} = \gamma_0^{(n)} \langle m \rangle^n \quad (27)$$

we find

$$\begin{aligned} \gamma_0^{(n)} &= 0 && \text{for operators } A \text{ with at least one } X_i \text{ or } Y_i \\ \gamma_0^{(n)} &= \delta_{n,m} && \text{for operators } A = Z_{i_1} Z_{i_2} \cdots Z_{i_m} \end{aligned} \quad (28)$$

For example, the operator  $X_i X_{i+1}$  can therefore *not* be proportional to  $m^2$  but its Taylor expansion starts with  $(\nabla m)^2$

$$\langle X_i X_{i+1} \rangle \sim \langle (\nabla m)^2 \rangle. \quad (29)$$

The same argument also shows that  $Z_i Z_{i+n} \approx m^2$  with prefactor 1 independent of  $n$ , as we will check numerically below.

## 2. Constraints arising from symmetries of the initial state

The initial state and the time evolution operator will typically not have the same symmetries. In all cases considered by us, there is, however, a subgroup of symmetries shared both by the initial state and the time evolution operator. Such symmetries remain intact throughout the time evolution and thus put extra strong constraints on the long-time dynamics.

(v) In our study, we consider only states which have a discrete translational invariance. A joint symmetry of initial state and time evolution are translations by either 2 or 4 sites,  $i \rightarrow i + 2n_0$  or, equivalently,  $x \rightarrow x + 2n_0 a$  in the field theory with  $n_0 = 1, 2$ . Therefore, only expectation values which carry integer multiples of the momentum  $\frac{\pi}{n_0 a}$  can be finite. Importantly, all operators with a finite momentum  $k_0$  decay exponentially within our effective field theory,  $\sim e^{-Dk_0^2 t}$ . Thus, to identify slowly decaying objects, we have to project each operator in the effective field theory to the zero-momentum sector. This is most easily done in momentum space. For example,  $(\nabla m)^2$  projected to zero momentum gives  $-\sum_{k_1 k_2} k_1 m_{k_1} k_2 m_{k_2} \delta(k_1 + k_2) = -\sum k^2 m_k m_{-k}$  where the projection is performed with the help of the  $\delta$  function. In contrast, all operators which are total derivatives like  $\nabla m^n$  or  $\nabla(m^{n_1} \nabla^{n_2} m^{n_3})$  vanish after projection [24] and thus cannot have a finite expectation value. Consider, for example  $\nabla m^2$ . In this case, projection gives  $\sum_{k_1 k_2} i(k_1 + k_2) m_{k_1} m_{k_2} \delta(k_1 + k_2) = 0$ . We can also prove this more generally. Consider a combination of fields  $A(x)$  which can be written as a total derivative,  $A(x) = \nabla B(x)$ . Any state with  $\langle A \rangle = \nabla \langle B(x) \rangle = \text{const.}$  thus features an expectation value  $\langle B(x) \rangle$  growing linearly in  $x$ , which is not possible in a translationally invariant system. Using the rules for powercounting, Eq. (14), the projection onto the zero-momentum sector and the symmetry arguments (ii) and (iii) we obtain the following table for leading operators in the zero-momentum sector

$R_{\pi \hat{x}}$	inversion $I_L$	selected leading operators
even	even	$m^2$ and $(\nabla m)^2$
	odd	$m^2 (\nabla m) (\nabla^2 m)$
odd	even	$m, m^3$ and $m(\nabla m)^2$
	odd	$(\nabla m)^3$

(vi) Our initial states have extra discrete symmetries jointly with the time evolution operator. For our arguments we need the following symmetries

$$\begin{aligned}
|\Psi_0^{(1)}\rangle &: R_{\pi \hat{x}} I_L \text{ and } R_{\alpha \hat{z}}, 0 \leq \alpha < 2\pi \\
|\Psi_0^{(2)}\rangle &: R_{\pi \hat{x}} \text{ and } I_L \\
|\Psi_0^{(3)}\rangle &: R_{\pi \hat{x}} R_{(\pi/2) \hat{z}} I_L
\end{aligned} \tag{31}$$

where, as above,  $I_L$  is the inversion on a link and  $R_{\alpha \hat{n}}$  is the rotation of all spins around the axis  $\hat{n}$ . Any operator either

in the bare theory or the continuum which is odd under this symmetry has to vanish. For example,  $\langle Z_1 Z_2 Z_3 \rangle$  vanishes exactly for all times for the initial state  $|\Psi_0^{(2)}\rangle$ , as it is odd under rotations around the  $\hat{x}$  axis by  $\pi$ .

In contrast,  $\langle Z_1 Z_2 Z_3 \rangle$  is finite for the initial state  $|\Psi_0^{(1)}\rangle$ , where initially  $\langle \Psi_0^{(1)} | Z_1 Z_2 Z_3 | \Psi_0^{(1)} \rangle = 1$ . Does this mean that  $\langle \int m^3(x) dx \rangle$  is finite in the continuum theory? The answer is negative as can be seen by a symmetry analysis.  $R_{\pi \hat{x}} I_L$  is a symmetry of the initial state  $|\Psi_0^{(1)}\rangle$  and of the time evolution. Thus, the expectation value of any operator which is even under inversion but odd under  $m \rightarrow -m$  has to vanish. This shows that  $\langle \int m^3(x) dx \rangle = 0$  or  $\langle \int m(x) (\nabla m(x))^2 dx \rangle = 0$ . Only terms which are odd in  $m$  and have an odd number of gradients can have a finite expectation value. The same argument applies also for the initial condition  $|\Psi_0^{(3)}\rangle$ , where, however, initially  $\langle \Psi_0^{(3)} | Z_1 Z_2 Z_3 | \Psi_0^{(3)} \rangle = 0$ . For the three different initial conditions, we therefore conclude

$$\begin{aligned}
\langle Z_1 Z_2 Z_3 \rangle^{(1)} &\sim (\nabla m)^3 \\
\langle Z_1 Z_2 Z_3 \rangle^{(2)} &= 0 \\
\langle Z_1 Z_2 Z_3 \rangle^{(3)} &\sim (\nabla m)^3.
\end{aligned} \tag{32}$$

(vii) Finally, there is one more property of the initial-state wave function, which we have to take into account, when discussing long-time tails: the precise form of the correlations of the initial state. As discussed in Eq. (16), the long-time tails arise when initial-state correlations of hydrodynamic modes differ from their final state correlations.

Most importantly, the leading-order long-time tail  $\sim 1/\sqrt{t}$  arises, as it takes a long time to build up the correlation  $\langle m(x)m(x') \rangle \approx \gamma \delta(x-x')$  in the long-time limit [25]. According to Eq. (16), this leading contribution *vanish*, if the correlations in the initial state  $C_{k=0}$  match correlations in the final state  $C_{k=0}^\eta / (2D_0)$ , as there is no need to redistribute magnetization in this case [25].

The final state of our system is indistinguishable from an infinite temperature state in the thermodynamics limit and therefore

$$\lim_{t \rightarrow \infty} \langle Z_i Z_j \rangle = \langle Z_i Z_j \rangle_{T=\infty} = \delta_{i,j}. \tag{33}$$

For our three initial states, we obtain

$$\begin{aligned}
\langle \Psi_0^{(1)} | Z_i Z_j | \Psi_0^{(1)} \rangle &= (-1)^{i+j} \\
\langle \Psi_0^{(2)} | Z_i Z_j | \Psi_0^{(2)} \rangle &= \langle \Psi_0^{(3)} | Z_i Z_j | \Psi_0^{(3)} \rangle = \delta_{i,j}.
\end{aligned} \tag{34}$$

Therefore, magnetization fluctuations of the initial state and final state are *identical* for the second and third initial conditions and we conclude that leading-order long time tails vanish in this case. For subleading terms, the situation is different. The initial and final states have, for example, a different expectation value of  $X_i X_{i+1}$ . As this operator has a finite overlap with the subleading term  $(\nabla m)^2$ , this implies that initial and final states are characterized by different values of  $\langle (\nabla m)^2 \rangle$ ,  $C_{k=0}'' \neq \frac{C_{k=0}''^\eta}{2D_0}$  in Eq. (16). Thus, we predict that

$$\langle Z_i Z_j \rangle^{(2,3)} \sim \frac{1}{t^{3/2}} \tag{35}$$

for the initial conditions  $|\Psi_0^{(2)}\rangle$  and  $|\Psi_0^{(3)}\rangle$ .

The same type of argument can also be applied to the  $m^4$  term. All expectation values  $\langle Z_i Z_j Z_k Z_l \rangle$  are identical in the initial and final state when starting from either  $|\psi_0^{(2)}\rangle$  or  $|\psi_0^{(3)}\rangle$  and therefore the leading long-time term  $\sim \frac{1}{t}$  vanishes in this case.

As a concrete example of how the seven rules are applied, consider the operator  $X_i Y_{i+1}$ . Applying rules (i-iii), we find after symmetrization that the operator is odd in  $m$  and odd under link-inversion

$$\begin{aligned} X_i Y_{i+1}|_{\text{sym}} &= \frac{1}{2}(X_i Y_{i+1} - Y_i X_{i+1}) \\ &\sim \nabla m + (\nabla m)m^2 + \nabla^3 m + \nabla \partial_t m \\ &\quad + (\nabla m)^3 + (\nabla m)(\partial_t m)m + \dots \end{aligned} \quad (36)$$

The terms are ordered according to their scaling dimension using  $m \sim t^{-1/4}$ ,  $\nabla \sim t^{-1/2}$ ,  $\partial_t \sim t^{-1}$ , see Eq. (14). Thus  $\nabla m$  appears to be the most relevant term. This is, however, *not* correct, as we have not taken into account the projection to the zero-momentum section (rule (v)). As all four terms in the second line of Eq. (36) are total derivatives, they vanish, when evaluated at  $P = 0$ . Thus, scaling predicts (omitting again prefactors) that

$$\langle X_i Y_{i+1} \rangle^{(1,3)} \sim \langle (\nabla m)^3 \rangle + \langle (\nabla m)(\partial_t m)m \rangle \quad (37)$$

provided that this term is allowed by the symmetry of the initial state, which is the case for the initial condition  $|\psi_0^{(1)}\rangle$  and  $|\psi_0^{(3)}\rangle$ .

### III. NUMERICAL RESULTS AND COMPARISON TO HYDRODYNAMICS

#### A. Computation of long-time tails

In our numerics, we consider systems with up to  $N = 28$  spins, where one can compute the time evolution defined in Eq. (2) ‘brute force’. After each time step, we compute the expectation value of all 255 observables, which can be defined on four neighboring sites. We follow the time evolution for typically 300 time steps starting from the initial conditions defined in Eq. (7). For longer times, finite size effects dominate and most expectation values are dominated by a finite-size background noise.

For the following comparison of numerics and analytics, we want to emphasize some limitations of our study. First, hydrodynamics is valid in the long-time limit only. The extremely slow decay,  $1/\sqrt{t}$ , of long-time correlations makes fits difficult as subleading terms are only suppressed by relative factors of  $1/\sqrt{t}$ . Thus, any observable has large subleading corrections. In practice, large corrections imply that we are not able to determine exponents by fits. Our goal is therefore not to ‘prove’ numerically that predictions from hydrodynamics are valid. Instead, we have a more modest goal: we show that the numerical data is consistent with the expectation from hydrodynamics. We are able to show this consistency for a huge set of observable. In a few cases, however,

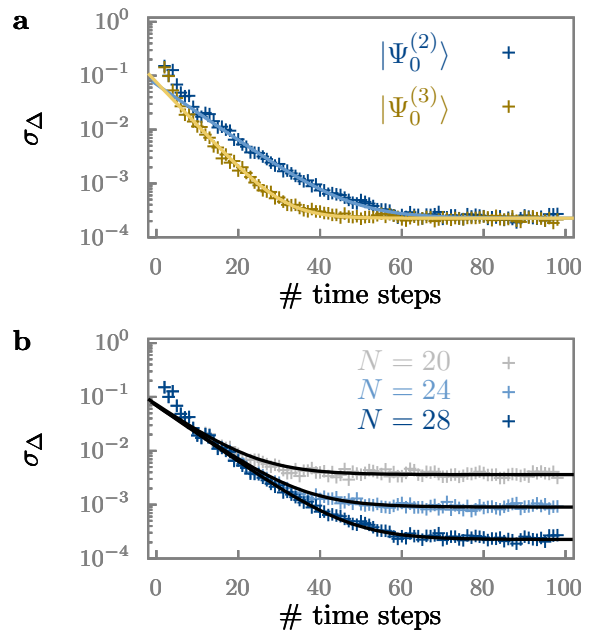


FIG. 1. Only operators symmetric under rotations around the  $z$  axis are protected by hydrodynamics and decay slowly, while the difference  $\langle A - A|_{\text{sym}} \rangle$  always decays exponentially. To test this assumption underlying our hydrodynamic analysis, we plot the standard-deviation  $\sigma_\Delta$  of this quantity averaged over all observables as defined in Eq. (38). The solid lines are fits to  $ae^{-t/\tau} + b2^{-N/2}$ , Eq. (41), with  $b \approx 3.7$ . The offset arises from finite-size effect and is approximately identical for the two initial conditions. Panel **a**: For the initial conditions  $|\psi_0^{(2)}\rangle$  and  $|\psi_0^{(3)}\rangle$ , we obtain from the fit  $\tau \approx 8.3$  and  $\tau \approx 5.4$ , respectively (for the initial condition  $|\psi_0^{(1)}\rangle$  one obtains  $\sigma_\Delta = 0$  by symmetry). The exponential decay also shows that the reduced density matrix of the subsystem approaches its symmetrized version with exponential precision, see Eq. (38). Panel **b**: The fit obtained from panel **a** describes (without readjusting fitting parameters) very well the data for  $N = 20$  and  $N = 24$ , thus confirming that the offset is exponentially suppressed for  $N \rightarrow \infty$ . Parameters for all figures:  $\alpha = 2$ ,  $\beta = 0.25$ ,  $\gamma = 1$ , and  $N = 28$  with the exception of two curves in panel **b**.

non-universal prefactors of the long-time tails are accidentally so small that possible power-law tails become indistinguishable from a pure exponential decay. After this disclaimer, we can now start to explore the validity of hydrodynamics in our model.

#### B. Exponentially fast decaying correlations

The most important assumption underlying the mapping to hydrodynamics is that all degrees of freedom, which are *not* protected by hydrodynamics, decay exponentially. This applies to all operators  $A - A|_{\text{sym}}$ , see Eq. (24) and Eq. (22).

To check this numerically, we compute this quantity for all 255 operators  $B_i$  considered by us and calculate the standard



deviation

$$\begin{aligned}\sigma_\Delta &= \left( \frac{1}{2^4} \sum_{i=1}^{255} \langle B_i - B_i|_{\text{sym}} \rangle^2 \right)^{1/2} \\ &= \| \rho^{\text{red}} - \rho^{\text{red}}|_{\text{sym}} \|.\end{aligned}\quad (38)$$

If and only if  $\langle B_i - B_i|_{\text{sym}} \rangle$  decays at least exponentially for all  $i$ , we can expect an exponential decay of  $\sigma_\Delta$ . Using Eq. (21), this quantity can also be identified with the operator norm (defined by  $\|A\| = (\frac{1}{2^4} \sum |A_{ij}^2|)^{1/2}$ ) of the difference of the reduced density matrix  $\rho^{\text{red}}$  of the subsystem and its symmetrized version.

In Fig. 1, we show this quantity. It decays exponentially but obtains a finite value for  $t \rightarrow \infty$ . To obtain an estimate for this offset, we consider the Lehmann representation of an operator  $A$

$$\langle A(t) \rangle = \sum_{nm} \langle \Psi_0 | n \rangle \langle n | A | m \rangle \langle m | \Psi_0 \rangle e^{i(\epsilon_n - \epsilon_m)t}. \quad (39)$$

The long-time limit is obtained from the fluctuations of the matrix elements [52]. For a completely random system with a Hilbert space of size  $2^N$ , each of the three matrix elements is estimated to be of order  $1/\sqrt{2^N}$ . The sum contains  $(2^N)^2$  terms of random sign. Therefore, we can estimate the size of the sum to be of order  $\sqrt{(2^N)^2}/(\sqrt{2^N})^3 \sim 2^{-N/2}$  with a random sign,

$$\langle A(t) \rangle \sim \pm 2^{-N/2} \quad \text{for } t \rightarrow \infty. \quad (40)$$

Therefore, we expect for large  $t$

$$\sigma_\Delta \approx a e^{-t/\tau} + b 2^{-N/2}. \quad (41)$$

The fit of Fig. 1, which was obtained for system size  $N = 28$  and could be applied to  $N = 20$  and  $N = 24$  without readjusting the fitting parameters, confirms this result with  $b \approx 3.7$  independent of  $N$ . The value of  $\tau$  depends on the initial conditions. For  $|\Psi_0^{(2)}\rangle$  and  $|\Psi_0^{(3)}\rangle$ , we obtain  $\tau \approx 8.3$  and  $\tau \approx 5.4$ , respectively. Apparently, the slowest exponentially decaying mode in the system with  $\tau \approx 8.3$  is only activated for the state  $|\Psi_0^{(2)}\rangle$ , see below.

From the 255 operators investigated by us, 128 have the property that they are odd under rotation around the  $z$  axis by  $\pi$ ,  $e^{-i\pi M_z/2} B_i e^{i\pi M_z/2} = -B_i$  and therefore  $B_i|_{\text{sym}} = 0$ . These operators only take a finite expectation value if the initial condition is not rotationally invariant, i.e., for  $|\psi_0^{(2)}\rangle$  and  $|\psi_0^{(3)}\rangle$ . In these cases we expect

$$\langle B_i(t) \rangle \approx \sum_j a_j e^{-\Gamma_j t} \cos(\omega_j t + \phi_j) + O(2^{-N/2}) \quad (42)$$

where the exponentially small offset is not a constant but a randomly oscillating function of time.

From our observables, we find that  $\langle X_i \rangle$  decays slowest for the initial condition  $|\Psi_0^{(2)}\rangle$  which has a finite net magnetization in the  $x$  direction. Apparently, its decay is the slowest

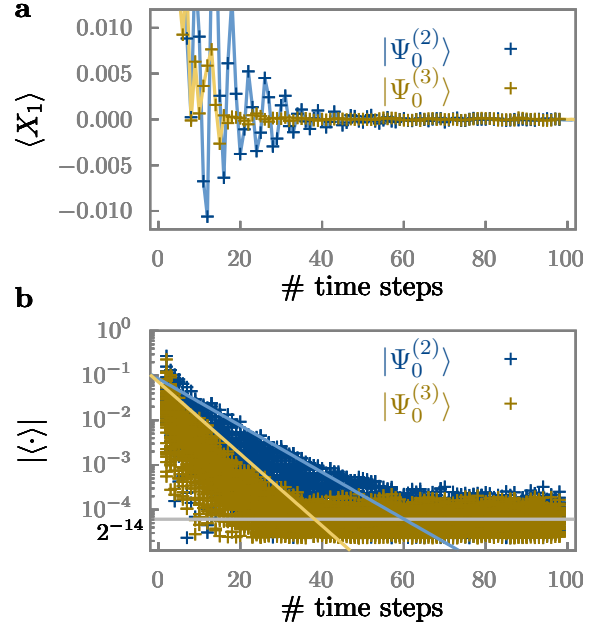


FIG. 2. Exponential decay of operators not protected by hydrodynamic modes. Panel a: Time dependence of  $\langle X \rangle$  for two different initial conditions,  $|\Psi_0^{(2)}\rangle$  and  $|\Psi_0^{(3)}\rangle$ . Panel b: Decay of 128 operators which are odd under rotations by  $\pi$  around the  $z$  axis and thus expected to decay exponentially. We plot the absolute value of the expectations for each operator in a log plot for two different initial states. Note that for the third initial state considered in this paper (staggered magnetization), the expectation values are exactly zero at all times. At long times the expectation values fluctuate around zero with amplitudes of order  $2^{-N/2}$  (gray line). The operators are decaying slower for the fully magnetized initial state (blue crosses) indicated by the light blue line compared to the state (yellow crosses) indicated by the light yellow line. The solid blue and yellow line denotes an exponential decay with the decay rates obtained from the fit in Fig. 1a.

exponentially decay mode in the system and is thus responsible for the longest relaxation time with  $\tau \approx 8.3$ . Fig. 2a shows that this slow decay occurs in combination with an oscillation. In Fig. 2b we analyze the decay of the expectation values of all 128 observables for which we predict an exponential decay in a logarithmic plot. The solid lines in Fig. 2b describes an exponential decay with the prefactor obtained from the fit to  $\sigma_\Delta$ , Eq. (41) to confirm that all quantities decay exponentially and that the fitted relaxation times indeed describes the slowest of the exponentially decaying modes. Thus, our best estimate for the local equilibration time is  $\tau_{\text{loc}} = \max \tau_i \approx 8.3$ , but strictly speaking,  $\sigma_\Delta$  and the quantities analyzed in this sections only probe operators perpendicular to the space of  $M_z$ -conserving, symmetrized operators.

In conclusion, our numerical results fully confirm that operators not protected by hydrodynamics decay exponentially.

### C. Long-time tails in $\langle Z_i Z_{i+n} \rangle$

Next, we investigate the decay of the slowest mode in the system,  $\langle Z_i Z_{i+n} \rangle$ .  $\langle Z_i Z_{i+n} \rangle$  is expected to decay asymptotically proportional to  $1/\sqrt{t}$ , as it has a finite overlap with  $m^2$  of the hydrodynamic theory, see Eq. (17). Fig. 3 shows that these expectation values indeed decay extremely slowly for an initial state with staggered magnetization,  $|\Psi_0^{(1)}\rangle$ . Even after 300 time steps, the observables have not yet reached a steady state. The expected decay exponent  $1/2$  can, however, not directly be determined by a fit as subleading corrections are too large. Subleading corrections to the  $1/\sqrt{t}$  behavior come from three different sources: finite size effects, non-linearities in the hydrodynamics field theory, and higher-order terms in the gradient expansion, see Eq. (16).

For a finite-size system with periodic boundary conditions and for  $t \gg N^2/D_0$ , the diffusion equation predicts an exponential decay of all correlations  $\sim e^{-D_0(2\pi/N)^2 t}$ . We have not tried to explore this long-time behavior in our numerics as our study wants to investigate long-time tails in the thermodynamic limit,  $N \rightarrow \infty$ . Nevertheless, fits have to take into account a possible finite offset. This offset is expected to be of order  $1/N$  which follows from scaling arguments: time scales proportional to the square of length in a diffusive system. Thus, we expect a  $1/N$  offset for an observable decaying with  $1/\sqrt{t}$ . The leading nonlinear term in the formula for the current, Eq. (10),  $D_2 m^2 \nabla m$  is suppressed by a factor  $m^2$  relative to the leading term  $-D_0 \nabla m$ . As  $m^2$  scales as  $1/\sqrt{t}$ , this gives rise to a relative correction of order  $1/\sqrt{t}$ , leading to a correction of order  $1/t$  to the expectation value of  $\langle Z_i Z_{i+n} \rangle$ . Finally, higher order corrections arise from higher order gradient terms either in the operator expansion or in the correlations of the initial state, see Eq. (16). Therefore, we conclude that

$$\langle Z_i Z_{i+n} \rangle^{(1)} \approx \frac{c_0}{N} + \frac{c_1}{\sqrt{t}} + \frac{c_2}{t} + \frac{\alpha_n}{t^{3/2}} + O\left(\frac{1}{t^2}\right). \quad (43)$$

Here, the prefactors  $c_0$ ,  $c_1$ ,  $c_2$  are expected to be independent of the distance  $n$  (for small  $n$ ), as they arise from zeroth-order gradient expansion and as there is a single slow mode in the field theory, the fluctuations of the local magnetization,  $m^2$ , which is responsible for this long-time tail. Physically, this long-time tail arises because it takes a long time to change these fluctuations by diffusive processes. In contrast,  $\alpha_n$  is different for different  $n$ . When performing a gradient expansion, the prefactor of the  $(\nabla m)^2$  term in Eq. (20) obviously depends on  $n$ , but one also has to take into account a contribution due to  $m \partial_t m$ . Both terms contribute to the  $1/t^{3/2}$  dependence at long times. In Fig. 3, the fits show that our numerical data is fully consistent with the prediction of Eq. (43). We expect that the long-time tails *vanish* if the correlations in the initial state match correlations in the final state (rule vi). Magnetization fluctuations of the initial state and final state are *identical* for the second and third initial conditions and we conclude that  $c_0 = c_1 = c_2 = 0$  in Eq. (43) in this case. Indeed,  $\langle Z_i Z_j \rangle$  takes much smaller numerical values in this case (not shown) and decays to a good approximation with  $1/t^{3/2}$ .

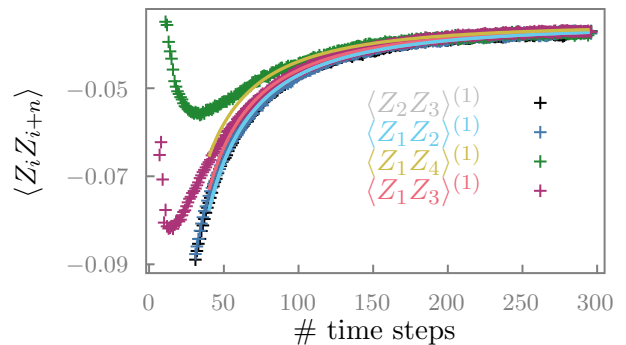


FIG. 3. Evolution of  $\langle Z_i Z_{i+n} \rangle$  after a quench as a function of time for the initial state  $|\psi_0^{(1)}\rangle$  (staggered magnetization). Dashed curves: Fitting function  $f(t) = \frac{c_0}{N} + \frac{c_1}{\sqrt{t}} + \frac{c_2}{t} + \frac{\alpha_i}{t^{3/2}}$ , Eq. (43), with  $\frac{c_0}{N} = -0.04$ ,  $c_1 = 0.2$ ,  $c_2 = -2.63$ ,  $\alpha_{\langle Z_1 Z_2 \rangle} = -1.05$ ,  $\alpha_{\langle Z_2 Z_3 \rangle} = -1.08$ ,  $\alpha_{\langle Z_1 Z_3 \rangle} = 0.11$ , and  $\alpha_{\langle Z_1 Z_4 \rangle} = 2.03$ . Here,  $c_1$  and  $c_2$  are set equal for all curves, see text.  $c_1$  is the standard hydrodynamic long-time tail,  $c_2$  arises from non-linear corrections in the diffusion equation. In contrast, the  $\sim 1/t^{3/2}$  dependence can originate from different modes (e.g., higher order gradient terms) that have distinct pre-factors. The fit shows, that the numerical result is consistent with the predictions from hydrodynamics but due to subleading terms and finite-size effects it is not possible to reliably extract exponents from the numerical data.

## IV. CONCLUSIONS AND OUTLOOK

For large classes of self-equilibrating many-particle quantum systems, the long-time dynamics of local observables is expected to be described by fluctuating hydrodynamics, i.e., by a classical field theory describing hydrodynamic modes and their fluctuations. Importantly, corrections to this theory decay exponentially, where the equilibration time remains finite in the thermodynamic limit. In contrast, hydrodynamic modes relax with powerlaws even in translationally invariant systems. We have put this theoretical framework to a test by (i) developing a set of analytical predictions for local observable and (ii) by showing that numerical simulations are consistent with the predictions from hydrodynamics for a large set of local observables.

An interesting question is what types of physical phenomena can *not* be captured within this framework. In the long-time limit, are there quantum properties not describable by purely classical fluctuating hydrodynamics? First, one obviously needs the full quantum theory to microscopically compute the parameters of the hydrodynamic theory like linear and non-linear diffusion constants. Second, the precise shape and time-dependence of finite-size corrections to observables, which we found to be exponentially suppressed with  $2^{-N/2}$ , are a finger-print of the quantum theory not accessible by the classical theory. But these corrections can safely be ignored in the thermodynamic limit. There are, however, quantities where this is not the case. One well-known and intensively studied [27–31] example is the entanglement entropy of the wave function computed for a large subsystem, e.g., of size  $N/2$ . The entanglement entropy grows linearly in time for

time scales which are linear in  $N$ . It tracks the quantum-scrambling of the many-particle wave function, which continues to grow on time scales much larger than any local equilibration time. Entanglement entropy is, however, extremely difficult to measure for large system sizes. An experiment, which may at least in principle be easier to realize on quantum computers, is a many-body echo experiment. After a time evolution  $U^n$  by  $n \gg 1$  steps governed by the time-evolution operator  $U$ , one can try to reverse the dynamics by applying  $U^\dagger$  gates

$$|\Psi\rangle \rightarrow |\Psi'\rangle = (U^\dagger)^n U^n |\Psi\rangle = |\Psi\rangle \quad (44)$$

for arbitrary  $n$ . As hydrodynamics contains dissipative terms with a well-defined arrow of time, one cannot capture the reversal of dynamics. In practice, however, small noise term or the small error in implementing  $U^\dagger$  can be expected to destroy the echo and the system will instead approach a thermal state for large  $n$ . Nevertheless, such many-body echo experiments (or, equivalently, the study of out-of-time correlation functions [32–35]) can be a powerful tool to reveal the presence of quantum correlations and their sensitivity to noise.

An important future project could be to explore the possibility to obtain a numerical algorithm which is able to efficiently compute the quench dynamics of large many-body quantum systems both for short and long times. Established numerical algorithms like exact diagonalization or DMRG require resources that scale exponentially with time, system size, or precision of the result. The observation that non-hydrodynamic quantities decay exponentially in time and the fact that classical field theories are easy to simulate give rise to the hope that - for the type of self-equilibrating systems studied in this

paper - algorithms may exist where computational costs scale with a power-law instead of exponentially. Indeed, Artiago *et al.* try to overcome the entanglement barrier in their recently proposed algorithm [53]. The algorithm exploits that local density matrices and, thus, physical observables are not influenced by the entanglement growth at large times and long-range entanglement and argues that such effects can be systematically discarded [53].

In conclusion, our study provides a detailed test of fluctuating hydrodynamics in a quantum system with a conservation laws. We are presently in the process to check the prediction of hydrodynamics for a broad set of local observables and we plan to provide an update of this study.

*Data availability:* We note that all raw data can be retrieved at Zenodo [54]. The data includes the time-series of the expectation values of all 255 operators. Each time series has 301 time steps. We provide the data for all three initial conditions and system sizes  $N = 20$ ,  $N = 24$  and  $N = 28$ . A mathematica notebook to create plots of the paper and beyond is provided as well. This notebook allows to explore the classification predicted in Tab. I and substitutes an appendix with  $3 \times 3 \times 255$  plots.

*Acknowledgements:* We thank Andreas Läuchli and Ivo Maceira for useful discussions and, especially, Luca Delacrétaz, who pointed out a major mistake in an earlier version of the manuscript. We acknowledge funding from the German Research Foundation (DFG) through CRC 183 (project number 277101999, A01 and B02) and – under Germany’s Excellence Strategy – by the Cluster of Excellence Matter and Light for Quantum Computing (ML4Q) EXC2004/1 390534769.

- 
- [1] A. Polkovnikov, K. Sengupta, A. Silva, and M. Vengalattore, Colloquium: Nonequilibrium dynamics of closed interacting quantum systems, *Reviews of Modern Physics* **83**, 863 (2011).
  - [2] J. Eisert, M. Friesdorf, and C. Gogolin, Quantum many-body systems out of equilibrium, *Nature Physics* **11**, 124 (2015).
  - [3] C. Gogolin and J. Eisert, Equilibration, thermalisation, and the emergence of statistical mechanics in closed quantum systems, *Reports on Progress in Physics* **79**, 056001 (2016).
  - [4] J. L. Lebowitz, E. Presutti, and H. Spohn, Microscopic models of hydrodynamic behavior, *Journal of Statistical Physics* **51**, 841 (1988).
  - [5] D. Forster, *Hydrodynamic Fluctuations, Broken Symmetry, and Correlation Functions (Frontiers in Physics)* (Westview Press, 1994) p. 352.
  - [6] T. Mori, T. N. Ikeda, E. Kaminishi, and M. Ueda, Thermalization and prethermalization in isolated quantum systems: a theoretical overview, *Journal of Physics B: Atomic, Molecular and Optical Physics* **51**, 112001 (2018).
  - [7] H. Spohn, *Large Scale Dynamics of Interacting Particles* (Springer Berlin Heidelberg, 1991).
  - [8] P. C. Martin, E. D. Siggia, and H. A. Rose, Statistical dynamics of classical systems, *Phys. Rev. A* **8**, 423 (1973).
  - [9] D. Forster, D. R. Nelson, and M. J. Stephen, Large-distance and long-time properties of a randomly stirred fluid, *Phys. Rev. A* **16**, 732 (1977).
  - [10] H. Spohn, Nonlinear fluctuating hydrodynamics for anharmonic chains, *Journal of Statistical Physics* **154**, 1191 (2014).
  - [11] L. Bertini, A. De Sole, D. Gabrielli, G. Jona-Lasinio, and C. Landim, Macroscopic fluctuation theory, *Reviews of Modern Physics* **87**, 593 (2015).
  - [12] H. Liu and P. Glorioso, Lectures on non-equilibrium effective field theories and fluctuating hydrodynamics, in *Theoretical Advanced Study Institute Summer School 2017” Physics at the Fundamental Frontier”*, Vol. 305 (Sissa Medialab, 2018) p. 008.
  - [13] K. Jensen, R. Marjeh, N. Pinzani-Fokeeva, and A. Yarom, A panoply of schwinger-keldysh transport, *SciPost Physics* **5**, 053 (2018).
  - [14] F. M. Haehl, R. Loganayagam, and M. Rangamani, Effective action for relativistic hydrodynamics: fluctuations, dissipation, and entropy inflow, *Journal of High Energy Physics* **2018**, 1 (2018).
  - [15] M. Crossley, P. Glorioso, and H. Liu, Effective field theory of dissipative fluids, *Journal of High Energy Physics* **2017**, 1 (2017).
  - [16] A. A. Michailidis, D. A. Abanin, and L. V. Delacrétaz, Corrections to diffusion in interacting quantum systems, *Physical Review X* **14**, 031020 (2024).
  - [17] L. V. Delacrétaz and R. Mishra, Nonlinear response in diffusive systems, *SciPost Physics* **16**, 047 (2024).

- [18] V. Popkov, A. Schadschneider, J. Schmidt, and G. M. Schütz, Exact scaling solution of the mode coupling equations for non-linear fluctuating hydrodynamics in one dimension, *Journal of Statistical Mechanics: Theory and Experiment* **2016**, 093211 (2016).
- [19] H. Spohn, The 1+1 dimensional Kardar–Parisi–Zhang equation: more surprises, *Journal of Statistical Mechanics: Theory and Experiment* **2020**, 044001 (2020).
- [20] B. Bertini, M. Collura, J. De Nardis, and M. Fagotti, Transport in out-of-equilibrium  $xxz$  chains: Exact profiles of charges and currents, *Phys. Rev. Lett.* **117**, 207201 (2016).
- [21] O. A. Castro-Alvaredo, B. Doyon, and T. Yoshimura, Emergent hydrodynamics in integrable quantum systems out of equilibrium, *Phys. Rev. X* **6**, 041065 (2016).
- [22] V. B. Bulchandani, R. Vasseur, C. Karrasch, and J. E. Moore, Solvable hydrodynamics of quantum integrable systems, *Phys. Rev. Lett.* **119**, 220604 (2017).
- [23] F. Hübner, E. Vernier, and L. Piroli, Generalized hydrodynamics of integrable quantum circuits, arXiv 10.48550/ARXIV.2408.00474 (2024), arXiv:2408.00474 [cond-mat.stat-mech].
- [24] S. Mukerjee, V. Oganesyan, and D. Huse, Statistical theory of transport by strongly interacting lattice fermions, *Phys. Rev. B* **73**, 035113 (2006).
- [25] J. Lux, J. Müller, A. Mitra, and A. Rosch, Hydrodynamic long-time tails after a quantum quench, *Physical Review A* **89**, 053608 (2014).
- [26] B. Bertini, F. Heidrich-Meisner, C. Karrasch, T. Prosen, R. Steinigeweg, and M. Žnidarič, Finite-temperature transport in one-dimensional quantum lattice models, *Rev. Mod. Phys.* **93**, 025003 (2021).
- [27] T. Rakovszky, F. Pollmann, and C. von Keyserlingk, Sub-ballistic growth of rényi entropies due to diffusion, *Physical Review Letters* **122**, 250602 (2019).
- [28] Y. Huang, Dynamics of rényi entanglement entropy in diffusive qudit systems, *IOP SciNotes* **1**, 035205 (2020).
- [29] T. Zhou and A. W. W. Ludwig, Diffusive scaling of rényi entanglement entropy, *Phys. Rev. Res.* **2**, 033020 (2020).
- [30] M. Žnidarič, Entanglement growth in diffusive systems, *Communications Physics* **3**, 100 (2020).
- [31] T. Rakovszky, F. Pollmann, and C. von Keyserlingk, Entanglement growth in diffusive systems with large spin, *Communications Physics* **4**, 91 (2021).
- [32] A. Bohrdt, C. B. Mendl, M. Endres, and M. Knap, Scrambling and thermalization in a diffusive quantum many-body system, *New Journal of Physics* **19**, 063001 (2017).
- [33] V. Khemani, A. Vishwanath, and D. A. Huse, Operator spreading and the emergence of dissipative hydrodynamics under unitary evolution with conservation laws, *Phys. Rev. X* **8**, 031057 (2018).
- [34] T. Rakovszky, F. Pollmann, and C. W. von Keyserlingk, Diffusive hydrodynamics of out-of-time-ordered correlators with charge conservation, *Phys. Rev. X* **8**, 031058 (2018).
- [35] G. Cheng and B. Swingle, Scrambling with conservation laws, *Journal of High Energy Physics* **2021**, 1 (2021).
- [36] A. J. Friedman, A. Chan, A. De Luca, and J. T. Chalker, Spectral statistics and many-body quantum chaos with conserved charge, *Phys. Rev. Lett.* **123**, 210603 (2019).
- [37] L. Capizzi, J. Wang, X. Xu, L. Mazza, and D. Poletti, Hydrodynamics and the eigenstate thermalization hypothesis, arXiv 10.48550/arxiv.2405.16975 (2024), arXiv:2405.16975 [quant-ph].
- [38] B. Ye, F. Machado, C. D. White, R. S. Mong, and N. Y. Yao, Emergent hydrodynamics in nonequilibrium quantum systems, *Physical Review Letters* **125**, 030601 (2020).
- [39] I. A. Maceira and A. M. Läuchli, Thermalization dynamics in closed quantum many body systems: a precision large scale exact diagonalization study, arXiv 10.48550/ARXIV.2409.18863 (2024), arXiv:2409.18863 [quant-ph].
- [40] S. Trotzky, Y.-A. Chen, A. Flesch, I. P. McCulloch, U. Schollwöck, J. Eisert, and I. Bloch, Probing the relaxation towards equilibrium in an isolated strongly correlated one-dimensional bose gas, *Nature Physics* **8**, 325 (2012).
- [41] A. M. Kaufman, M. E. Tai, A. Lukin, M. Rispoli, R. Schittko, P. M. Preiss, and M. Greiner, Quantum thermalization through entanglement in an isolated many-body system, *Science* **353**, 794 (2016).
- [42] S. Erne, R. Bücker, T. Gasenzer, J. Berges, and J. Schmiedmayer, Universal dynamics in an isolated one-dimensional bose gas far from equilibrium, *Nature* **563**, 225 (2018).
- [43] Z.-Y. Zhou, G.-X. Su, J. C. Halimeh, R. Ott, H. Sun, P. Hauke, B. Yang, Z.-S. Yuan, J. Berges, and J.-W. Pan, Thermalization dynamics of a gauge theory on a quantum simulator, *Science* **377**, 311 (2022).
- [44] U. Schneider, L. Hackermüller, J. P. Ronzheimer, S. Will, S. Braun, T. Best, I. Bloch, E. Demler, S. Mandt, D. Rasch, and A. Rosch, Fermionic transport and out-of-equilibrium dynamics in a homogeneous hubbard model with ultracold atoms, *Nature Physics* **8**, 213 (2012).
- [45] C. Zu, F. Machado, B. Ye, S. Choi, B. Kobrin, T. Mittiga, S. Hsieh, P. Bhattacharyya, M. Markham, D. Twitchen, A. Jarmola, D. Budker, C. R. Laumann, J. E. Moore, and N. Y. Yao, Emergent hydrodynamics in a strongly interacting dipolar spin ensemble, *Nature* **597**, 45 (2021).
- [46] J. F. Wienand, S. Karch, A. Impertro, C. Schweizer, E. McCulloch, R. Vasseur, S. Gopalakrishnan, M. Aidelsburger, and I. Bloch, Emergence of fluctuating hydrodynamics in chaotic quantum systems, *Nature Physics* **10.1038/s41567-024-02611-z** (2024).
- [47] I. M. Georgescu, S. Ashhab, and F. Nori, Quantum simulation, *Rev. Mod. Phys.* **86**, 153 (2014).
- [48] Y. Yang, A. Christianen, S. Coll-Vinent, V. Smelyanskiy, M. C. Bañuls, T. E. O’Brien, D. S. Wild, and J. I. Cirac, Simulating prethermalization using near-term quantum computers, *PRX Quantum* **4**, 030320 (2023).
- [49] J. Richter, O. Lunt, and A. Pal, Transport and entanglement growth in long-range random clifford circuits, *Phys. Rev. Res.* **5**, L012031 (2023).
- [50] C. Jonay, J. F. Rodriguez-Nieva, and V. Khemani, Slow thermalization and subdiffusion in  $u(1)$  conserving floquet random circuits, *Phys. Rev. B* **109**, 024311 (2024).
- [51] X. Turkeshi, P. Calabrese, and A. De Luca, Quantum mpemba effect in random circuits, arXiv preprint arXiv:2405.14514 (2024).
- [52] M. Srednicki, The approach to thermal equilibrium in quantized chaotic systems, *Journal of Physics A: Mathematical and General* **32**, 1163 (1999).
- [53] C. Artiago, C. Fleckenstein, D. Aceituno Chávez, T. K. Kvornring, and J. H. Bardarson, Efficient large-scale many-body quantum dynamics via local-information time evolution, *PRX Quantum* **5**, 020352 (2024).
- [54] A. Matthies, N. Dannenfeld, S. Pappalardi, and A. Rosch, Data for "Thermalization and hydrodynamic long-time tails in a Floquet system" [Data set], Zenodo 10.5281/zenodo.13939642 (2024).